A model proposed by Efrima and Bixon[28] and others[29,30] amends eq 11 by considering the Franck–Condon factors for vibrational transitions. This theory leads to the prediction that excited vibrational states of the ground electronic product state are formed for reactions where $\Delta G + \lambda < 0$. In terms of eq 11, energy from available product vibrational modes, E_v, is added to the electronic-ground-state free energy change of the reaction until $\Delta G + E_v + \lambda = 0$. The significance of these quantum effects could be experimentally tested by comparing the absorption decays of excited singlet states with the growth of their respective cations' absorptions.

In the formulations of eq 5, used to obtain the electron-transfer rate constants, and eq 11, relating the rate of electron transfer to free energy and solvent reorganization changes, a distribution of reactants and products is neglected. Both equations assume reactants at an encounter distance, R. The best fit R values listed for TS/FN and DMES/FN in Table II correspond to center-to-center edge-on contact van der Waals radii between these two sets of reactants. If the larger R values listed for reactant sets TS/TCE and DMES/TCE are valid, eqs 5 and 11 would not be explicitly applicable. A more general representation of electron-transfer reactions includes radial[20,31] and geometrical[32] distributions of reactants and products. For a reaction at $r = R$, involving neutral reactants, large relative to the solvent, the bimolecular rate constant given in eq 11 follows from eq 12.

$$k_{et} = \kappa \int_R^\infty (\exp[-\alpha(r - R)])(\exp[-\Delta G^*(r)/kT])r^2\, dr \qquad (12)$$

Consistent with eq 11, $\Delta G^*(r) = [(\lambda(r) + \Delta G)^2/4\lambda]$, and κ is approximately[31] 10^{13} M^{-1} s^{-1}. The contributions to the observed k_{et} from reactions at $r > R$ will then obviously depend on the values of α, about 2 $Å^{-1}$ [33], and ΔG.

The radial and, depending on the shape of the reactants, geometrical dependences of the reorganization energy are due to the solvent.[31] In the normal region ($\lambda + \Delta G > 0$), the maximum rate constant is produced when solvent molecules are perturbed minimally during the reaction. This would correspond to the reactants forming contact ion pairs[7,34] at $r = R$, where the local change in dielectric constant would not be as great as if two separate ions were independently solvated, as in the case of solvent-separated ion pairs. When this argument is extended to the inverted region ($\lambda + \Delta G < 0$), contributions to the observed rate from reactants at $r > R$ become important as $\lambda(r) + \Delta G \rightarrow 0$. Classically, the preference for long-range electron transfer in solution may be influenced therefore by values of ΔG, $d\lambda(r)/dr$, and the ratio k_d/k_{et}, in addition to the effective solvent dielectric constant mentioned above. A study of the radial distribution of product states initially created in the electron-transfer reactions as a function of free energy change, solvent polarity, and viscosity is therefore of interest. In a previous communication,[7a] we reported the predominant formation of contact ion pairs in the reaction of TS and FN in acetonitrile. We have not yet employed this technique to study the systems TS/TCE and DMES/TCE in acetonitrile or other solvents.

Acknowledgment. This work was supported by the National Science Foundation (Grant CHE 8418611).

Registry No. AN, 107-13-1; FN, 764-42-1; TCE, 670-54-2; TS, 103-30-0; DMES, 18869-29-9.

(28) Efrima, S.; Bixon, M. *Chem. Phys.* **1976**, *13*, 447.
(29) Dogonadze, R. R.; Kuznetsov, A. M.; Vorotyntsev, M. A. *Phys. Status Solidi B* **1972**, *54*, 125.
(30) Schmickler, W. *J. Chem. Soc., Faraday Trans. 2* **1976**, *72*, 307.
(31) Marcus, R. A. *Int. J. Chem. Kinet.* **1981**, *13*, 865.
(32) Siders, P.; Cave, R. J.; Marcus, R. A. *J. Chem. Phys.* **1984**, *81*, 5613.
(33) Jortner, J. *J. Chem. Phys.* **1976**, *64*, 4860.
(34) Winstein, S.; Robinson, G. C. *J. Am. Chem. Soc.* **1958**, *80*, 169.

Microcanonical Variational Theory of Radical Recombination by Inversion of Interpolated Partition Function, with Examples: $CH_3 + H$, $CH_3 + CH_3$

Wendell Forst

Laboratoire de Physicochimie Théorique, URA 503, Université de Bordeaux I, 33405 Talence Cedex, France
(Received: July 24, 1990)

A simple interpolation scheme involving the logarithms of partition functions for initial and final states in a bond-fission reaction is used to represent, as a function of distance along the reaction coordinate, the total partition function for the transition state. The inverse Laplace transform of this partition function yields a distance-dependent state count for the transition state that serves as input for a variational routine incorporated into a standard RRKM calculation. In this way, the number of states of so-called transitional modes, in particular, is made to connect smoothly with the proper number of states of fragment rotations. The interpolation makes use of simple Morse potential for the breaking bond and one of two similar S-type switching functions: a one-parameter Gaussian and a two-parameter hyperbolic tangent, either of which gave similar results for the title recombinations, in essential agreement with experiment. It is shown that the negative temperature coefficient of a radical recombination arises primarily from the above types of switching functions, which cause a "late" switch (i.e., at large interfragment distance) to product configuration.

1. Introduction

It is generally agreed that locating the transition state (TS, properties of which are denoted by asterisk) at the centrifugal maximum of the effective potential in simple bond-fission unimolecular reactions (reactions where the reverse radical association proceeds without an energy barrier) is not the best choice since it leads to difficulties associated with the rate constant for radical association at low temperatures.[1] To alleviate this problem, a microcanonical variational criterion is now employed,[2] defined as the local minimum in $G^*(E^*,r)$, the total number of states of TS along the reaction coordinate:

$$dG^*(E^*,r)/dr = 0 \qquad (1)$$

where r is the distance along the reaction coordinate and E^* is the internal randomizable energy of the transition state (cf. eq 26). If the solution of eq 1 for a local minimum is $r = r_{min}$, then the property of interest is $G^*(E^*,r_{min})$, understood to be evaluated at $r = r_{min}$.

(1) Hase, W. L.; Wardlaw, D. M. In *Bimolecular Collisions*; Ashfold, M. N. R., Baggott, J. E., Eds.; Royal Society of Chemistry: London, 1989; Chapter 4.
(2) Wardlaw, D. M.; Marcus, R. A. *Adv. Chem. Phys.* **1987**, *70*, 231.

0022-3654/91/2095-3612$02.50/0

The consequence of eq 1 is that attention must be paid to structural changes of the reactant in the course of the dissociation. In the simplest implementation of eq 1, vibrational modes of the reactant that undergo a substantial change of character during the decomposition (so-called "transitional" modes) are made dependent on the distance r along the reaction coordinate via the empirical relation[3]

$$\nu(r) = \nu_e S(r) \tag{2}$$

where $\nu(r)$ is the now r-dependent mode frequency and $S(r)$ is a switching function such that $S(r_e) = 1$ and $S(\infty) = 0$; the subscript e refers to equilibrium value of distance r at potential minimum. The remaining modes, which are not directly involved in the decomposition, are termed "conserved" modes.

In its simplest form $S(r)$ is assumed to be an exponential function[4] of r:

$$S(r) = \exp[-\alpha(r - r_e)] \tag{3}$$

with α an adjustable parameter. The problem with eq 3, noted before,[5] is that as $r \to \infty$, $S(r) \to 0$, and therefore also $\nu(r) \to 0$; hence $G^*(E^*)$ tends to go off to infinity at large r. However transitional modes in bond-fission reactions connect with fragment rotations, the number of states of which is therefore being overcounted.

The purpose of this work is to propose a relatively simple interpolation scheme that connects, at specified E^*, the number of states of transitional vibrational modes, of frequency ν_e at $r = r_e$, with the correct number of states of fragment rotations at $r \to \infty$. The scheme involves only a minor modification of an existing routine and is therefore readily implemented and incorporated into a variational treatment.

2. Density of Sum of States by Inversion of the Partition Function

It is well-known[6] that a smooth-function approximation to the density (or sum) of states can be obtained by taking the inverse Laplace transform of the partition function, an approximation that performs well down to very low energies.[7] Given below is a brief outline of the method.

With $s = 1/kT$ the transform parameter, let the total partition function of the system of interest be $Q(s)$ and let E be the energy at which the density or sum of states is to be calculated. The complex inversion integral is then

$$I(k) = \frac{1}{2\pi i}\int_{c-i\infty}^{c+i\infty} \frac{Q(s)e^{sE}\,ds}{s^k} \tag{4}$$

where the path of integration is a straight line parallel to the imaginary axis with abscissa c. $I(k=0)$ represents $N(E)$, the density of states at E, and $I(k=1)$ represents $G(E)$, the total number of states (or state count for short) at E:

$$G(E) = \int_0^E N(E)\,dE$$

The integrand in eq 4 is generally sharply peaked and therefore can be approximated by the method of steepest descents. It is convenient to work with the logarithm of the integrand in eq 4, $\phi(z)$, where $z = \exp(-s)$:

$$\phi(z) = \ln Q(z) - k \ln (\ln z^{-1}) - E \ln z \tag{5}$$

The integrand will have a saddle point at some $z = \theta$, and if the integrand is expanded around θ to first order, it can be shown that

$$I(k) = \frac{Q(\theta)}{[\ln \theta^{-1}]^k \theta^E [2\pi\theta^2\phi''(\theta)]^{1/2}} \tag{6}$$

where $\phi''(\theta)$ is the second derivative of $\phi(z)$ evaluated at $z = \theta$.

Inasmuch as the method involves only manipulations of the partition function, the minimization problem in eq 1 is therefore "solved" if one can set up an r-dependent partition function by means of an interpolation scheme that provides a proper interpolation between reactant transitional modes and the product rotations with which they connect.

3. Logarithmic Interpolation Formula

For reasons that will appear shortly, consider an interpolation scheme for transitional modes (subscript t) involving the *logarithms* of partition functions.[8] If $Q_{m,t}$ is the partition function of the transitional modes in the reactant molecule, and $Q_{p,rot}$ the partition function of product rotations that correlate with transitional modes, then the (natural) logarithm of the corresponding partition function in TS (Q^*) is assumed to evolve with distance r according to

$$\ln Q^*_t(r) = [(\ln Q_{m,t}) - (\ln Q_{p,rot})]S(r) + \ln Q_{p,rot} \tag{7}$$

where the switching function $S(r)$ is for the moment arbitrary.

Extending this scheme to "conserved" degrees of freedom (subscript c), regardless of whether they actually undergo a change of frequency as they evolve from reactant to products, we can write quite generally

$$\ln Q^*_c(r) = [(\ln Q_{m,c}) - (\ln Q_{p,c})]S(r) + \ln Q_{p,c} \tag{8}$$

where $Q_{m,c}$ is the partition function for conserved modes in the reactant molecule, and $Q_{p,c}$ is the partition function for conserved modes in the products. Combining eqs 7 and 8, we have

$$\ln Q^*_{tot}(r) = (\ln Q_{m,tot})S(r) + (\ln Q_{p,tot})[1 - S(r)] \tag{9}$$

where subscripts tot refer to all degrees of freedom in the transition state (*), the molecule (subscript m), or the products (subscript p), *exclusive* of the reaction coordinate and the two overall degrees of freedom of rotation involved in E_{rot} (eq 25). The term "all" degrees of freedom will be used henceforth in this narrowed sense.

In the present context, eq 9 is particularly convenient since the function $\phi(z)$ in eq 5 is likewise defined in terms of the logarithm of the total partition function of the system. For separable degrees of freedom—the usual assumption in conventional RRKM calculations, and implicit in the separation of modes between "conserved" and "transitional"—the logarithmic representation has the additional advantage that the logarithm of the total partition function of the system is then merely a sum of terms, one for each degree of freedom.

4. Application to a Sum-of-States Calculation for Transition State

Although eq 9 is quite general and applicable to any system for which one can write down a partition function, to apply eq 6 to the calculation of r-dependent $G^*(E^*)$ in eq 1 we shall make the simplifying assumption that vibrational modes are harmonic and rotations are free and classical, as is usual in conventional RRKM calculations. In terms of the variable z, the general form of the vibrational partition function Q_v is

$$Q_v = \prod_k (1 - z^{\omega_k})^{-1} \tag{10}$$

where ω_k is the frequency (in cm^{-1}) of the kth mode. To distinguish the original vibrational modes of the reactant molecule (excluding the reaction coordinate) from those of the products, index i will designate those of the molecule and index j those of the products. Thus, for example, index i will run from 1 to $3N - 6$ or $3N - 7$ (N = number of atoms in molecule), depending on whether molecule is linear or nonlinear. The rotational partition function for r classical rigid free rotors is similarly

$$Q_r = q_r/(\ln z^{-1})^{r/2} \tag{11}$$

where $q_r = Q_r/(kT)^{r/2}$, i.e., q_r is the kT- (or z-) independent factor, including the appropriate symmetry number. In this representation

(3) Hase, W. L. *J. Chem. Phys.* **1976**, *64*, 2442.
(4) Quack, M.; Troe, J. *Ber. Bunsen-Ges. Phys. Chem.* **1974**, *78*, 240.
(5) Davies, J. W.; Pilling, M. J. In *Bimolecular Collisions*; Ashfold, M. N. R., Baggott, J. E., Eds.; Royal Society of Chemistry: London, 1989; Chapter 3.
(6) Forst, W. *Theory of Unimolecular Reactions*; Academic Press: New York, 1973; Chapter 6 and Appendix. Hoare, M. R.; Ruijgrok, T. W. *J. Chem. Phys.* **1970**, *52*, 113. Yau, A. W.; Pritchard, H. O. *Can. J. Chem.* **1977**, *55*, 992.
(7) Forst, W.; Prasil, Z. *J. Chem. Phys.* **1969**, *51*, 3006.
(8) Quack, M.; Troe, J. *Ber. Bunsen-Ges. Phys. Chem.* **1977**, *81*, 329.

an r-dimensional rotation counts for r rotors.

We now have to distinguish between r_a = the number of "active" free rotors and r_t = the number of product rotors that arise from transitional modes in the molecule. The first kind are rotors that contribute to the density or sum of states in the reactant molecule (e.g., the K rotor in the symmetric top, which correlates with one fragment rotation); their number r_a remains constant throughout the decomposition, and only q_r changes with distance along the reaction coordinate from $q_{r,m}$ (in the molecule, at r_e) to $q_{r,p}$ (in the products, at $r \rightarrow \infty$). This change is accomplished by interpolation of the appropriate logarithms and is implicit in eq 9:

$$\ln q_r = (\ln q_{r,m})S(r) + (\ln q_{r,p})[1 - S(r)] \quad (12)$$

The second kind are the r_t rotors (with their own q_{rt}, which does not change with distance) that appear only in the products. Since all degrees of freedom must be accounted for in the reactant molecule and the products, we have

$$(\sum_i 1) + r_a = (\sum_j 1) + r_a + r_t \quad (13)$$

To find the saddle point in the integrand of eq 4, we have to solve the transcendental equation $\phi'(z) = 0$. From eq 5 we have

$$z\phi'(z) = \sum_i \frac{\omega_i z^{\omega_i}}{1 - z^{\omega_i}} S(r) + \frac{k + r_a/2}{\ln z^{-1}} + \left(\sum_j \frac{\omega_j z^{\omega_j}}{1 - z^{\omega_j}} + \frac{r_t/2}{\ln z^{-1}} \right)[1 - S(r)] - E^* = 0 \quad (14)$$

where E^* is the internal distributable energy of the transition state. Note that in eq 14 all the q_r have dropped out. The root of this equation is readily found by the Newton–Raphson method. If z_1 is the initial estimate, then the next (better) estimate is $z_2 = z_1 - [z_1\phi'(z_1)]/\phi''(z_1)$, where $\phi''(z_1)$ is the second derivative evaluated at $z = z_1$:

$$\phi''(z) = \sum_i \frac{\omega_i^2 z^{\omega_i - 1}}{(1 - z^{\omega_i})^2} S(r) + \frac{k + r_a/2}{z(\ln z^{-1})^2} + \left(\sum_j \frac{\omega_j^2 z^{\omega_j - 1}}{(1 - z^{\omega_j})^2} + \frac{r_t/2}{z(\ln z^{-1})^2} \right)[1 - S(r)] \quad (15)$$

This procedure is repeated until $|z_2 - z_1|$ is sufficiently small; then the last $z_2 = \theta$.

For substitution into the final equation for the (now distance dependent) sum of states of the transition state (eq 6 with $k = 1$ and $E = E^*$), we need the complete r-dependent transition-state partition function $Q^*(r)$ evaluated at $z = \theta$. For the molecule, let

$$L_m = (\ln q_{r,m}) - \sum_i \ln (1 - \theta^{\omega_i}) \quad (16)$$

and for the products let

$$L_p = (\ln q_{r,p}) + \ln \frac{q_{r,t}}{(\ln \theta^{-1})^{r_t/2}} - \sum_j \ln (1 - \theta^{\omega_j}) \quad (17)$$

Then

$$Q^*(r,\theta) = \frac{\exp\{L_m S(r) + L_p[1 - S(r)]\}}{(\ln \theta^{-1})^{r_a/2}} \quad (18)$$

The one element still needed in eq 6 is the second derivative (eq 15), which is already available from the last iteration.

5. Switching Function $S(r)$

It is obvious that a simple exponential form of $S(r)$, as in eq 3, will produce from transitional modes modified according to eq 2 a state count $G^*(E,r)$ that is different from one obtained by inversion of the logarithm of the partition function of eq 9. This is shown in Figure 1 (upper panel) for the specific case ($CH_4 \rightarrow CH_3 + H$, where the circles indicate the actual initial and final values of the state count $G^*(E,r)$ at $r = r_e$ [for CH_4] and at $r \rightarrow \infty$ [for $CH_3 + H$], respectively, at the stated constant energy. [In the actual variational calculation, the energy is of course not constant as a function of r, since $G^*(E,r)$ "rides" on the rising portion of the effective potential, with the result that $G^*(E,r)$ goes through a minimum.] The dashed line is the state count based on eq 2 and a Morse representation of the C–H bond, using, in eq 3, $\alpha = \beta(\text{Morse})/2$, which appears to be a near-"universal" relation[9] for the switching function of eq 3. This line tends to go off to infinity for $r \rightarrow \infty$, as could be expected. The continuous lines are state counts based on eq 9, using the same exponential form of $S(r)$ (eq 3), for three different values of the parameter α. Clearly the dashed and continuous lines are of completely different character, so that there is no value of α that would make them coincide.

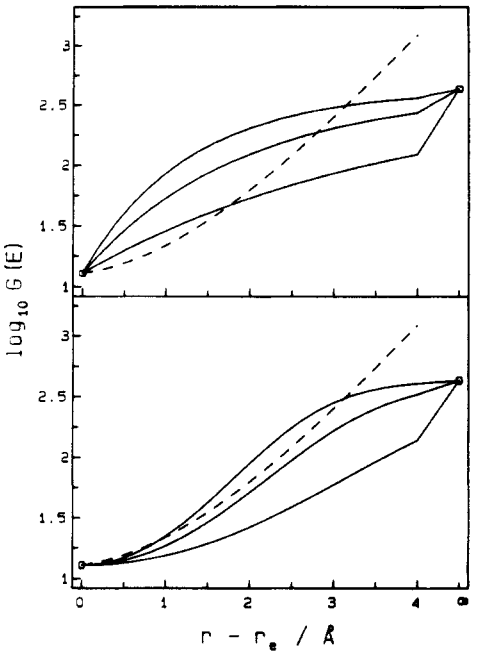

Figure 1. Interpolation of r dependence of state count $G(E)$ for the case $CH_4 \rightarrow CH_3 + H$ at $E = 1000$ cm^{-1}. Upper panel: dashed line, $G(E)$ calculated from r-dependent frequencies (eq 2) using exponential form of $S(r)$ (eq 3) with $\alpha = 0.8691$ Å^{-1}; continuous lines, $G(E)$ calculated by inversion from eq 9, by using exponential form of $S(r)$ (eq 3), with, top to bottom, $\alpha = 0.75$, 0.5, and 0.25 Å^{-1}. Lower panel: dashed line, same as above; continuous lines, $G(E)$ calculated by inversion from eq 9, by using hyperbolic tangent form of $S(r)$ (eq 19) with, top to bottom, $b = 2$, and $a = 0.15$, 0.1, and 0.05 Å^{-2}. In both panels circles indicate the actual initial and final values of $G(E)$ at $r - r_e = 0$ and $r - r_e \rightarrow \infty$, respectively. Both panels have a common horizontal axis.

The exponential form of the switching function (eq 3) is inspired by empirical relations that relate bond order or force constant to bond extension, such as Pauling's or Badger's rules.[10] As a result, it can be expected that this form of $S(r)$, as used in eq 2, will give a reasonable r dependence of vibrational frequencies (and therefore reasonable r dependence of state count) at moderate bond extensions but not at large ones; an ab initio calculation[11] more or less confirms this. To make the state count based on eq 9 return comparable and therefore presumably more realistic, results at small r, it is therefore of interest to find a form of $S(r)$ that would give r dependence of $G^*(E,r)$ similar to that obtainable from eqs 2 and 3 at small r, while at the same time reaching to the correct limiting value at iarge r.

One such form is the two-parameter hyperbolic tangent function

$$S(r) = 1 - \tanh [a(r - r_e)^b] \quad (19)$$

where a and b are constants such that b determines the curvature,

(9) Troe, J. *Z. Phys. Chem.* (Munich) **1989**, *161*, 209.
(10) Pauling, L. *The Nature of the Chemical Bond*, 3rd ed.; Cornell U. Press: Ithaca, NY, 1960. Herschbach, D. R.; Laurie, V. W. *J. Chem. Phys.* **1961**, *35*, 458.
(11) Merkel, A.; Zulicke, L. *Mol. Phys.* **1987**, *60*, 1379.

i.e., whether approach to final ($r \to \infty$) value is "early" or "late", while the constant a (dimension distance^{-b}) determines roughly the slope at midrange for specified b. Another form is the one-parameter Gaussian function

$$S(r) = \exp[-c(r - r_e)^2] \tag{20}$$

where the constant c has the dimension distance^{-2}. Both functions have a very similar S shape. This is shown in Figure 1 (lower panel) for the hyperbolic tangent with $b = 2$ and three different values of a. The dashed line represents the result of the same exponential form of $S(r)$ (eq 3) applied to frequencies (eq 2) as in the upper panel of Figure 1. At small r, a reasonable match between the two representations is obtained for $a = 0.1$ Å^{-2} at $E = 1000$ cm^{-1}; a similar match at a different energy would require only slightly different values of a and b.

The Gaussian function of eq 20 with $c \approx 0.07$, 0.13, and 0.20 Å^{-2} will produce results very similar to those of the lower panel of Figure 1 representing the hyperbolic tangent function with $a = 0.05$, 0.1, and 0.15 Å^{-2}, respectively. In the following, all calculations using the partition function inversion approach will make use of the switching functions of eq 19 and/or eq 20.

6. Zero-Point Energy and the Variational Treatment

The specification of E^* requires attention to zero-point energy. As transitional vibrational modes are converted into rotations, their zero-point energy "disappears", i.e., is converted into distributable energy (E^* in eq 14) since there is no zero-point energy in a free rotor. A simple way to take this into account is to define a partition function for the zero-point energy of the reactant molecule (all modes, reaction coordinate excepted):

$$Q_{z,m} = \exp(-\epsilon_{zm}/kT) \tag{21}$$

where $\epsilon_{zm} = {}^1/_2\sum_i \omega_i$, and similarly a partition function for the (total) zero-point energy $Q_{z,p}$ of the products, with the summation in ϵ_{zp} running over index j of the product frequencies. The logarithms of Q_z are then interpolated in the usual fashion to obtain the corresponding r-dependent partition function for the zero-point energy of the transition state $Q^*_z(r)$:

$$\ln Q^*_z(r) = (\ln Q_{z,m})S(r) + (\ln Q_{z,p})[1 - S(r)] \tag{22}$$

This is equivalent to

$$\epsilon^*_z(r) = \epsilon_{zm}S(r) + \epsilon_{zp}[1 - S(r)] \tag{23}$$

where $\epsilon^*_z(r)$ is the r-dependent zero-point energy of the transition state. Thus the interpolation of the zero-point energies proceeds in the same way as the interpolation of the logarithms of the partition functions.

Since $\epsilon_{zm} > \epsilon_{zp}$, conversion of vibrations into rotations increases the distributable energy E^* in the transition state with increasing r, at constant total energy E of the decomposing molecule. However this is taken into account in the usual variational treatment: let $V_{eff}(r)$ be the effective potential at r, given by

$$V_{eff}(r) = V(r) + E_{rot}(r_e/r)^2 \tag{24}$$

where $V(r)$ is the vibrational potential and E_{rot} is the rotational energy of the reactant molecule given by

$$E_{rot} = J(J + 1)B_e \tag{25}$$

The approximation implicit in eqs 24 and 25 is that the decomposition is viewed as the fragmentation of a quasi-diatom XY into X + Y, where X and Y are polyatomic fragments. Thus B_e in eq 25 is, in principle, the equilibrium value of the rotational constant of XY, and J is the rotational quantum number, a conserved quantity throughout the decomposition. In practice, if the decomposing molecule is, e.g., a symmetric top, B_e is taken to be one of the two equal rotational constants, and the component of rotational energy associated with the rotational quantum number K is considered an active degree of freedom contributing to state count.

At specified J and with energy zero for $V(r)$ at potential minimum, E^*, the internal distributable energy of the transition state relative to its own ground state is then

$$E^* = E - V_{eff}(r) - \epsilon^*_z(r) + \epsilon_{zm} + E_{rot} \tag{26}$$

where E is the total internal distributable energy above the ground state of the reacting molecule. As a result, the E^* that appears in eq 14 and in the final expression for $G^*(E^*) \equiv I(k{=}1)$ in eq 6 is also r dependent. Similarly, the reaction will have an r- and J-dependent threshold energy $E_J(r)$:

$$E_J(r) = V_{eff}(r) - E_{rot} + \epsilon^*_z(r) - \epsilon_{zm} \tag{27}$$

Combining eqs 26 and 27, we see that

$$E^* = E - E_J(r) \tag{28}$$

The minimization of $G^*(E^*,r)$ from eq 1 then proceeds by choosing a collection of r's for every specified E and J and picking out, at $r = r_{min}$, the smallest $G^*(E^*,r)$ by a convenient routine. The microcanonical rate constant $k(E,J)$ for dissociation at specified E and J is then given by the standard RRKM formula:

$$k(E,J) = \frac{G^*(E^*,r_{min})}{hN(E)} \tag{29}$$

where $N(E)$ is the density of states of the reactant molecule at E. The J dependence of $k(E,J)$ arises via eq 24.

With $k(E,J)$ given by eq 29, the pressure-dependent rate constant for decomposition at specified J will be represented by the standard RRKM expression:

$$k_{uni}(J) = \frac{1}{Q_m}\int_0^\infty \frac{\omega k(E,J)\, N(E) \exp(-E/kT)\, dE}{\omega + k(E,J)} \tag{30}$$

where

$$Q_m = \int_0^\infty N(E) \exp(-E/kT)\, dE$$

is the partition function for all vibrational degrees of freedom of the molecule (including the reaction coordinate), plus r_a rotors. The lower limit of the integral is, in effect, $E_J(r_{min})$. To keep the focus on the variational rather than weak-collision aspects, ω will be interpreted for simplicity as the effective collision frequency: thus we shall use $\omega \approx \beta_{wc}Z_{LJ}p$, where β_{wc} is a weak-collision correction factor, Z_{LJ} is the Lennard-Jones collision number and p is pressure. More elaborate weak-collision treatments are available.[12,13]

7. A Simplified Version

Since r_{min} is energy dependent (cf. lower panel in Figure 4), $E_J(r_{min})$ is likewise energy dependent but generally only weakly so (cf. lower panel in Figure 2). If the energy dependence of $E_J(r_{min})$ is ignored, then in the limit of high pressure ($\omega \to \infty$), eq 30 reduces to

$$k_\infty(J) = \frac{\exp[-E_J(r_{min})/kT]}{hQ_m}\int_0^\infty G^*(E^*,r_{min})e^{-E^*/kT}\, dE^* \tag{31}$$

by making use of eqs 28 and 29. However

$$\int_0^\infty G^*(E^*,r_{min}) \exp(-E^*/kT)\, dE^* = kTQ^*_{tot}(r_{min}) \tag{32}$$

where $Q^*_{tot}(r_{min})$ is the minimized partition function whose logarithm is defined in eq 9. Thus eq 31 becomes

$$k_\infty(J) = \frac{kT}{h}\frac{\exp[-E_J(r_{min})/kT]Q^*_{tot}(r_{min})}{Q_m} \tag{33}$$

The simplification that this equation represents compared with the limiting form of eq 30 at $\omega \to \infty$ is that (at a given T) it requires only a minimization of $\exp[-E_J(r)/kT]Q^*_{tot}(r)$ at every J, rather than the minimization of $G^*(E^*,r)$ at every E and J.

(12) Smith, S. C.; Gilbert, R. G. *Int. J. Chem. Kinet.* **1988**, *20*, 307.
(13) Forst, W. *J. Phys. Chem.* **1989**, *93*, 3145.

TABLE I: Calculated Canonical J-Averaged Thermal Rate Constants for the Recombination $CH_3 + H \rightarrow CH_4$[a]

	switching function (this work)							
	hyperbolic tangent			Gaussian			AW[b]	
T, K	$\langle k_{rec,0}\rangle$	$\langle k_{rec,\infty}\rangle$	$\langle r_{min}\rangle$	$\langle k_{rec,0}\rangle$	$\langle k_{rec,\infty}\rangle$	$\langle r_{min}\rangle$	$\langle k_{rec,\infty}\rangle$	$\langle r_{min}\rangle$
300	3.17	4.57	4.05	2.79	4.65	4.29	2.57	3.7
400	2.19	4.51	3.94	2.01	4.98	4.16	2.84	3.5
600	1.15	4.13	3.77	1.09	5.07	3.96	3.29	3.3
800	0.650	3.75	3.63	0.628	4.92	3.80	3.42	3.2
1000	0.385	3.45	3.52	0.376	4.73	3.67	3.60	3.1

[a] tanh switching function (eq 19) with $a = 0.084$ Å$^{-2.2}$, $b = 2.2$. Gaussian switching function (eq 20) with $c = 0.151$ Å^{-2}. All $\langle k_{rec,0}\rangle$ in 10^{-29} cm^6/molecules^2 s (including $\beta_{wc} = 0.04$). All $\langle k_{rec,\infty}\rangle$ in 10^{-10} cm^3/molecules s. $\langle r_{min}\rangle$ is the J-averaged position of the transition state in angstroms. [b] AW: FTST calculation of Aubanel and Wardlaw.[20] $\langle k_{rec,\infty}\rangle$ corresponds to k_C^{cl} from their Table VII, $\langle r_{min}\rangle$ corresponds to their R_T from Table IX.

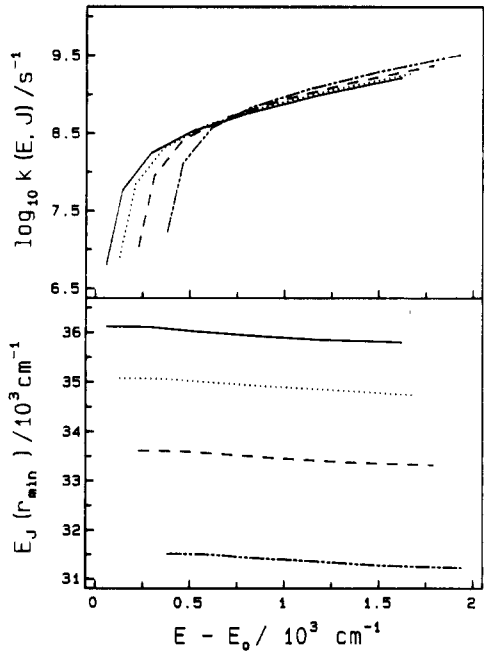

Figure 2. Upper panel: energy dependence of microcanonical rate constant $k(E,J)$ for the *dissociation* $CH_4 \rightarrow CH_3 + H$ at several J, using the hyperbolic tangent switching function (eq 19) with $a = 0.084$ Å$^{-2.2}$, $b = 2.2$. Left to right, the curves are for $J = 0$ (continuous line), 14 (dotted line), 22 (dashed line), and 30 (dot-dashed line). Lower panel: Same calculation as above, showing the energy dependence of the minimized critical energy for decomposition $E_J(r_{min})$ (eq 27 for $r = r_{min}$) at $J = 0$ (continuous line), 14 (dotted line), 22 (dashed line), and 30 (dot-dashed line). Both panels have a common horizontal axis, E_0 is the threshold energy at $J = 0$, $r \rightarrow \infty$.

At the low-pressure limit, dissociation occurs as soon as the minimum energy for reaction is reached, so that the transition state is located at the top of the zero-point energy corrected effective potential. If this maximum is at $r = r_{max}$, the critical energy for decomposition is $E_J(r=r_{max})$, given by eq 27. The rate constant is then

$$k_0(J) = \frac{\beta_{wc} Z_{LJ} \exp[-E_J(r=r_{max})/kT]}{Q_m} \times \int_0^\infty N[E + E_J(r=r_{max})] e^{-E/kT}\, dE \quad (34)$$

This equation yields results identical with those obtainable from eq 30 in the limit $\omega \rightarrow 0$, at considerable saving in machine time.

The J-averaged rate constants for recombination at the high- and low-pressure limits then follow via the equilibrium constant and eq 36.

8. Example 1: Recombination $CH_3 + H \rightarrow CH_4$

As one example of the results obtainable with the described interpolation routine, presented below is a brief summary of the calculation of the rate constant for the association reaction $CH_3 + H \rightarrow CH_4$, which has received much attention in the literature and may be considered a useful test case.

The present calculation used a simple Morse potential for $V(r)$ in eq 24 with $\beta = 1.7382$ Å^{-1} obtained from the standard relation

$$\beta = 2\pi c\omega(\mu/2D)^{1/2} \quad (35)$$

where c = speed of light, ω = energy (cm^{-1}) of the vibrational degree of freedom that becomes the reaction coordinate (C–H stretch), μ = reduced mass of the CH_3 and H moieties, and D = classical height of the bare barrier. All molecular parameters for reactant and products were taken from Tables VII and VIII in Pilling et al.[14] Note that, since in the present approach it is the *total* partition function that is interpolated (eq 9), it is not necessary to make a distinction between conserved and transitional modes, only between r_a and r_t rotors.

Microcanonical rate constants for dissociation were calculated from eq 27 at several E and fixed J, as input for 15-point Gauss–Laguerre integration of the thermal rate constant $k_{uni}(J)$ (eq 30), which was then transformed into the recombination rate constant $k_{rec}(J)$ via the equilibrium constant. This calculation was repeated for a sufficiently large collection of J's (0–78 in the present case) to permit averaging over $P(J)$, the thermal distribution of J's:

$$\langle k_{rec}\rangle = \sum_J P(J)\, k_{rec}(J) \quad (36)$$

where $P(J) = (2J + 1)\exp(-E_{rot}/kT)$.

Figure 2 gives the results of the microcanonical calculations for the decomposition $CH_4 \rightarrow CH_3 + H$ using the hyperbolic tangent form for $S(r)$ (eq 19) with $a = 0.084$ Å$^{-2.2}$ and $b = 2.2$, which gave the best overall results. The upper panel illustrates the energy dependence of the rate constant $k(E,J)$ at several fixed J, as a function of $E - E_0$, where E_0 is the critical energy for $J = 0$ at $r \rightarrow \infty$ (i.e., the enthalpy of the reaction at 0 K). The lower panel shows (for the same selection of J's) that the energy dependence of the critical energy $E_J(r_{min})$ is indeed weak, and thus justifies the development that leads to eq 33.

Figure 3 shows the calculated falloff of the J-averaged rate constant $\langle k_{rec}\rangle$ for the recombination $CH_3 + H \rightarrow CH_4$ at 300 and 600 K, calculated from eq 30, using $\beta_{wc} = 0.04$ throughout. This calculation is compared with the experimental results of Pilling et al. (symbols) for falloff in the presence of helium (ref 14, Table I). Considering that helium is a particularly weak collider, the weak-collision factor $\beta_{wc} = 0.04$ used in the calculation seems reasonable.

Table I summarizes the results on the temperature dependence of the rate constant $\langle k_{rec,\infty}\rangle$ calculated from the canonical expression in eq 33, as well as the corresponding average location of the transition state along the reaction coordinate, defined as

$$\langle r_{min}\rangle = [\sum_J r_{min}(J)\, k_{rec,\infty}(J)\, P(J)]/\langle k_{rec,\infty}\rangle \quad (37)$$

where $r_{min}(J)$ is the location of the minimum of $\exp(-E_J(r)/kT)Q^*_{tot}(r)$ at a given J. Also included for comparison are results obtained with the gaussian switching function (eq 20) using $c = 0.151$ Å^{-2}.

Pilling et al.[14] found the limiting high-pressure rate constant for recombination to be essentially temperature independent in

(14) Brouard, M.; Macpherson, M. T.; Pilling, M. J. *J. Phys. Chem.* **1989**, *93*, 4047.

TABLE II: Calculated Canonical J-Averaged Thermal Rate Constants for the Recombination $CH_3 + CH_3 \rightarrow C_2H_6$[a]

	switching function (this work)							
	hyperbolic tangent			Gaussian			WM[b]	
T, K	$\langle k_{rec,0}\rangle$[c]	$\langle k_{rec,\infty}\rangle$	$\langle r_{min}\rangle$	$\langle k_{rec,0}\rangle$[c]	$\langle k_{rec,\infty}\rangle$	$\langle r_{min}\rangle$	$\langle k_{rec,\infty}\rangle$	$\langle r_{min}\rangle$
300	2.05E-26	6.23	4.37	2.21E-26	6.69	4.29	8.43	4.2
500	3.80E-27	5.34	4.04	3.97E-27	5.26	3.97	7.27	3.8
1000	1.70E-28	3.21	3.59	1.73E-28	2.81	3.52	4.63	3.4
2000	1.88E-30	1.76	3.20	1.89E-30	1.40	3.14	2.19	3.0

[a] tanh switching function (eq 19) with $a = 0.28$ Å$^{-1.51}$, $b = 1.51$. Gaussian switching function (eq 20) with $c = 0.2625$ Å^{-2}. All $\langle k_{rec,0}\rangle$ in cm^6/molecules^2 s (including $\beta_{wc} = 0.1$ throughout). All $\langle k_{rec,\infty}\rangle$ in 10^{-11} cm^3/molecules s. $\langle r_{min}\rangle$ is the J-averaged position of the transition state in angstroms. [b] WM: FTST calculation of Wardlaw and Marcus (ref 21, Table VII). $\langle k_{rec,\infty}\rangle$ and $\langle r_{min}\rangle$ correspond to their k_∞^{III} and R_{III}, respectively. [c] 2.05E-6 = 2.05×10^{-6}.

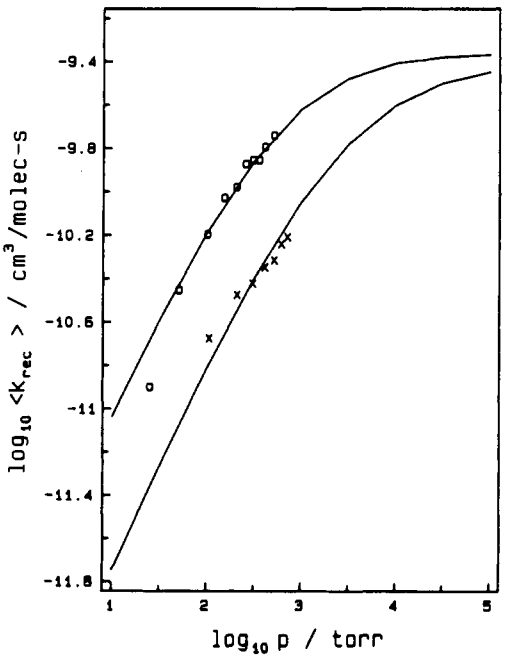

Figure 3. Calculated falloff of $\langle k_{rec}\rangle$ for the *association* $CH_3 + H \rightarrow CH_4$ at 300 and 600 K, by using the hyperbolic tangent switching function (eq 19) with $a = 0.084$ Å$^{-2.2}$, $b = 2.2$ (continuous lines). Symbols are experimental results of Pilling et al. (ref 22, Table I) in the presence of helium heat bath at 300 (circles) and 600 K (crosses). Calculation used weak collision factor $\beta_{wc} = 0.04$ at both temperatures.

the range 300–400 K. A review by Tsang and Hampson[15] of both low-temperature recombination and high-temperature dissociation data recommends an overall negative temperature coefficient in the range 300–2500 K: $\langle k_{rec,\infty}\rangle = 2.06 \times 10^{-10}(T/298)^{-0.4}$ (units those of Table I). An earlier review by Warnatz[16] recommends an even larger overall negative temperature coefficient (T^{-1}) in the same temperature range.

A summary of a number of calculations of the canonical average $\langle k_{rec,\infty}\rangle$ at a single temperature (300 K) and of various degrees of sophistication but using the Morse function, may be found in Cobos:[17] in general, the calculated $\langle k_{rec,\infty}\rangle$ varies between 4×10^{-10} and 7×10^{-10}, the lowest value being a more recent result of Pacey et al.[18] (units are those of Table I). According to Pilling,[14] the best experimental result is $\langle k_{rec,\infty}\rangle = 4.7 \times 10^{-10}$ at 300 K, not far from the result shown in Table I.

The calculated results in Table I for the Gaussian switching function show for $\langle k_{rec,\infty}\rangle$ a positive temperature coefficient between 300 and 600 K, which becomes negative at higher temperatures. On the other hand, the hyperbolic tangent switching function produces a slowly increasing *negative* temperature coefficient from almost zero ($\approx T^{-0.05}$) in the 300–400 K range to $\approx T^{-0.38}$ in the 800–1000 K range. Microcanonical variational calculations on the $CH_3 + H$ system were done previously by Hase et al.,[19] and more recently by Aubanel and Wardlaw[20] using the "flexible transition-state theory" (FTST), the canonical version of which is shown in the last two columns of Table I. Both calculations report for $\langle k_{rec,\infty}\rangle$ a *positive* temperature coefficient in the range 300–2500 K.

At the low-pressure limit, optimized calculations of Pilling et al.[14] using the "energy-grained master equation" approach yielded $\langle k_{rec,0}\rangle = 2.48 \times 10^{-29}$, compared with the experimental value of 4×10^{-29} (helium heat bath at 300 K; units of Table I). These may be compared with the calculated results obtained for $\langle k_{rec,0}\rangle$ in this work, as shown in Table I at a number of temperatures, using the same weak-collision factor throughout.

9. Example 2: The Recombination $CH_3 + CH_3 \rightarrow C_2H_6$

This reaction has also received much attention in the literature, both experimentally and theoretically, and represents therefore another useful test case. The calculation using the present inversion approach proceeded in much the same way as for the recombination $CH_3 + H$. Thus a Morse function was used for the interfragment potential $V(r)$, with $\beta = 1.806$ Å^{-1} calculated from eq 35, while molecular parameters were taken from Wardlaw and Marcus.[21] Owing to the larger masses involved, calculations were done for a collection of J's between 0 and 204.

Both the hyperbolic tangent (eq 19) and Gaussian (eq 20) switching functions were used, with $a = 0.28$ Å$^{-1.51}$, $b = 1.51$ in the first case, and $c = 0.2625$ Å^{-2} in the second. Both gave similar results, with the hyperbolic switching function yielding a somewhat smaller negative temperature coefficient. This may be seen in Table II, which summarizes results obtained in the present calculation for the canonical rate constants $\langle k_{rec,0}\rangle$ and $\langle k_{rec,\infty}\rangle$. For comparison, the last two columns show results of FTST calculations of Wardlaw and Marcus.[21]

Figure 4 shows the results of microcanonical calculations for the decomposition $C_2H_6 \rightarrow CH_3 + CH_3$ using the Gaussian switching function. The upper panel illustrates the energy dependence of the rate constant $k(E,J)$ at several fixed J, as a function of $E - E_0$, while the lower panel illustrates the energy dependence of r_{min} for the same collection of J's.

Insofar as experimental results are concerned, there are reviews by Tsang and Hampson,[15] who recommend for the experimental temperature dependence of the high-pressure rate constant $\langle k_{rec,\infty}\rangle = 4.38 \times 10^{-11}(T/298)^{-0.64}$ in the range 300–2500 K, and by Warnatz,[16] who recommends $\langle k_{rec,\infty}\rangle = 4.08 \times 10^{-11}(T/298)^{-0.40}$ in the range 300–2000 K (units are those of Table II). Recently extensive experimental data over a range of pressures and temperatures by Gutman et al.[22] became available for the $CH_3 + CH_3$ association. Figure 5 compares the Gutman data (symbols) with the J-averaged $\langle k_{rec}\rangle$ obtained in the present microcanonical calculation (continuous lines) at 296, 474, and 906 K, using a temperature-independent $\beta_{wc} = 0.1$.

(15) Tsang, W.; Hampson, R. F. *J. Phys. Ref. Data* **1986**, *15*, 1087.
(16) Warnatz, J. In *Combustion Chemistry*; Gardiner, W. C., Jr., Ed.; Springer-Verlag: New York, 1984.
(17) Cobos, C. J. *J. Chem. Phys.* **1986**, *85*, 5644, Table I.
(18) King, S. C.; LeBlanc, J. F.; Pacey, P. D. *Chem. Phys.* **1988**, *123*, 329.
(19) Hase, W. L.; Mondro, S. L.; Duchovic, R. J.; Hirst, D. M. *J. Am. Chem. Soc.* **1987**, *109*, 2916.
(20) Aubanel, E. E.; Wardlaw, D. M. *J. Phys. Chem.* **1989**, *93*, 3117, Table VIII.
(21) Wardlaw, D. M.; Marcus, R. A. *J. Phys. Chem.* **1986**, *90*, 5383; erratum, *Ibid.* **1987**, *91*, 4864.
(22) Slagle, I. R.; Gutman, D.; Davies, J. W.; Pilling, M. J. *J. Phys. Chem.* **1988**, *92*, 2455.

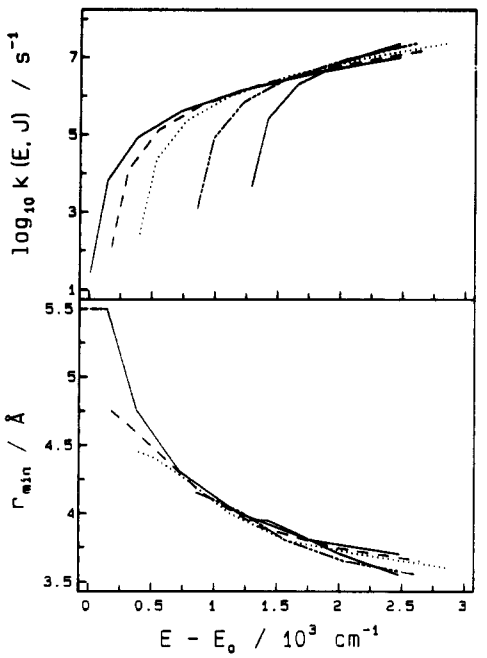

Figure 4. Upper panel: energy dependence of microcanonical rate constant $k(E,J)$ for the *dissociation* $C_2H_6 \rightarrow CH_3 + CH_3$, at (left to right) $J = 0$ (continuous line), $J = 50$ (dashed line), $J = 74$ (dotted line), $J = 104$ (double-dot dashed line) and $J = 124$ (continuous line), by using the Gaussian switching function (eq 20) with $c = 0.2625$ Å^{-2}. Lower panel: same calculation as above, showing the energy dependence of r_{min} at the same selection of J's, with the same identification of lines. Both panels have a common energy axis. E_0 = threshold energy at $J = 0$, $r \rightarrow \infty$.

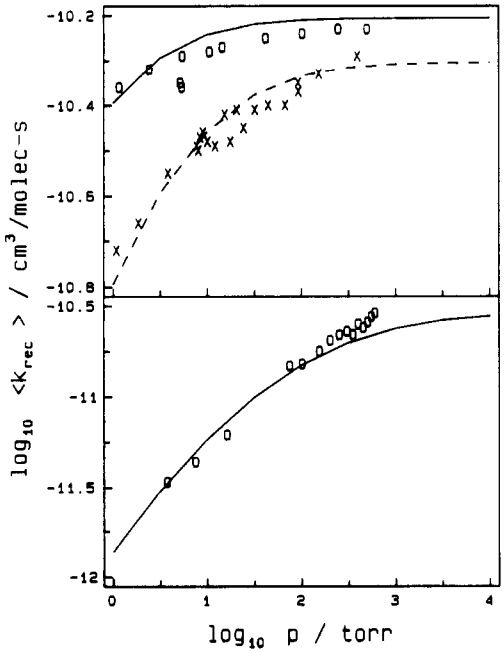

Figure 5. Calculated falloff (lines) of $\langle k_{rec} \rangle$ for the *association* $CH_3 + CH_3 \rightarrow C_2H_6$ in the presence of argon as heat bath, at three temperatures, using the Gaussian switching function (eq 20) with $c = 0.2625$ Å^{-2}. Symbols are experimental results of Gutman et al. (ref 22, Tables I and II). Upper panel: continuous line and circles, 296 K, dashed line and crosses, 474 K. Lower panel: 906 K. Calculation used $\beta_{wc} = 0.1$ at all three temperatures. Both panels have a common pressure axis.

10. Discussion

The results of the microcanonical calculations show the expected features of the E and J dependence of the rate constant $k(E,J)$ (top panels in Figures 2 and 4), as well as of $E_J(r_{min})$ (Figure 2, bottom); in particular, r_{min} (Figure 4, bottom) illustrates clearly how the transition state "tightens" with increasing energy, i.e., moves to shorter internuclear distances. The calculated falloffs of $\langle k_{rec} \rangle$ (Figures 3 and 5) compare quite well with experiment,

TABLE III: Comparison of Microcanonical (μcan, Eq 30) and Canonical (can, Eq 33) Calculations of $\langle k_{rec,\infty} \rangle$

	switching function			
	hyperbolic tangent, eq 19		Gaussian, eq 20	
T, K	μcan	can	μcan	can
	Association $CH_3 + H \rightarrow CH_4$[a]			
300	4.34	4.57	4.57	4.65
600	3.91	4.13	4.94	5.07
	Association $CH_3 + CH_3 \rightarrow C_2H_6$[b]			
296	5.84	6.55	6.18	6.72
474	5.09	5.47	4.97	5.45

[a] $\langle k_{rec,\infty} \rangle$ in units of 10^{-10} cm^3/molecules s. tanh switching function (eq 19) with $a = 0.084$ Å$^{-2.2}$, $b = 2.2$. Gaussian switching function (eq 20) with $c = 0.151$ Å^{-2}. [b] $\langle k_{rec,\infty} \rangle$ in units of 10^{-11} cm^3/molecules s. tanh switching function (eq 19) with $a = 0.28$ Å$^{-1.51}$, $b = 1.51$. Gaussian switching function (eq 20) with $c = 0.2625$ Å^{-2}.

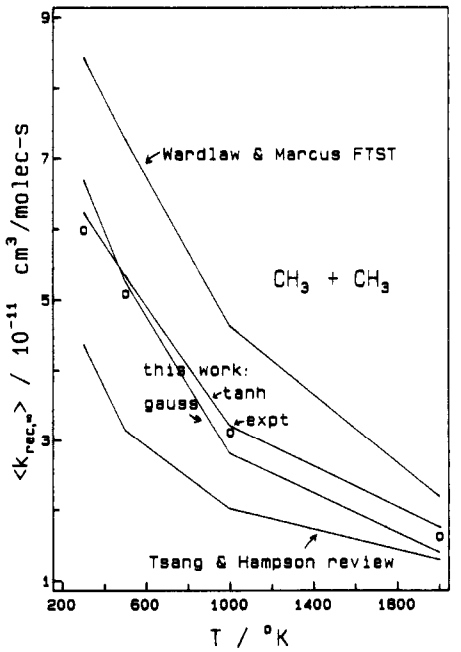

Figure 6. Summary of data on the temperature dependence of $\langle k_{rec,\infty} \rangle$ for the association $CH_3 + CH_3$. Experiment: Tsang and Hampson review;[15] "expt" (circles, ref 23 and Table IV). Theory: Wardlaw and Marcus FTST,[21] this work (Table II).

given the crude allowance for weak-collision effects via the factor β_{wc} which appears to have a reasonable value for CH_4 + helium ($\beta_{wc} = 0.04$) and a slightly higher value for C_2H_6 + argon ($\beta_{wc} = 0.1$); both are roughly temperature independent over the limited temperature range involved, as is usual.

The temperature coefficient of the recombination rate constant, which is perhaps a more sensitive test of the theory than the falloff, is best discussed in terms of $\langle k_{rec,\infty} \rangle$, which is readily accessible from the canonical expression in eq 33. Since this expression represents merely an upper limit, it is useful first to determine the deviation of the canonical expression from the high-pressure limit of $\langle k_{rec} \rangle$ as determined from the microcanonical eq 30, which is shown in Table III. In the $CH_3 + H$ recombination the difference shown is only about 5% for the hyperbolic tangent switching function and about 2% for the Gaussian switching function. In the methyl radical recombination, due to a not-quite-so-weak an energy dependence of $E_J(r_{min})$, the canonical rate constant exceeds the microcanonical $\langle k_{rec,\infty} \rangle$ by a larger margin, about 10%, but even this deviation is not larger than estimated experimental error in the rate constants. These deviations may be compared with a 20% difference reported by Wardlaw and Marcus[21] using the FTST.

In the case of the recombination $CH_3 + CH_3$, recent experiments, not-so-recent reviews of experimental data over a wide temperature range, and theory (including this work) all agree that

TABLE IV: Theoretical Fit to Experiment in the Recombination $CH_3 + CH_3 \rightarrow C_2H_6$ (Argon Collider)

T, K	$\langle k_{rec,0} \rangle^a$	$\langle k_{rec,\infty} \rangle^b$
300	3.28E-26[c]	5.98E-11
500	5.77E-27	5.08E-11
1000	1.77E-28	3.11E-11
2000	2.72E-30	1.62E-11

[a] Calculated from $k_0 = 8.76 \times 10^{-7} T^{-7.03} e^{-1390/T}$ cm^6/molecules^2 s. Data of Wagner and Wardlaw,[23] eq 5. [b] Calculated from $k_\infty = 1.5 \times 10^{-7} T^{-1.18} e^{-329/T}$ cm^3/molecules s. Data of Wagner and Wardlaw,[23] eq 5. [c] 3.28E-26 = 3.28×10^{-26}.

the rate constant $\langle k_{rec,\infty} \rangle$ has a negative temperature coefficient from about room temperature upward, as summarized graphically in Figure 6. In fact, the results presented in section 9 are quite comparable to those obtained by the FTST, even including the location of the transition state (Table II). The computed values of the canonical rate constants compare quite well with the theoretical fit to the Gutman experimental data obtained by Wagner and Wardlaw[23] (WW) (Table IV), a fit that in the case of $\langle k_{rec,0} \rangle$ includes weak-collision effects. The comparison of the present results in Table II with those in Table IV is fairly good even for the low-pressure rate constant $\langle k_{rec,0} \rangle$ with temperature-independent $\beta_{wc} = 0.1$.

The recombination $CH_3 + H$ presents a different picture. Recent experiments suggest temperature invariance of $\langle k_{rec,\infty} \rangle$ over a limited temperature range (300–400 K), while reviews of experimental data over a wide temperature range indicate a negative temperature coefficient. Previous implementations of the variational routine, on the other hand, all produced a positive temperature coefficient in the range 300–2500 K; this is shown graphically in Figure 7.

It is therefore interesting to note that in the present work it was not possible to model the temperature dependence of the $CH_3 + H$ association over the *entire* range of temperatures with the one-parameter Gaussian switching function—that is, if one assumes that the reaction has a temperature coefficient that goes from about zero around 300–400 K to a progressively more negative value at higher temperatures. For any reasonable value of the constant c, the Gaussian switching function returned consistently a small *positive* temperature coefficient in a small interval near 300–400 K, a coefficient that became progressively more *negative* at higher temperatures (cf. Table I and Figure 7).

This is in contrast with the $CH_3 + CH_3$ recombination, where there was no difficulty in finding constant c that would yield roughly the desired (negative) temperature coefficient. The greater flexibility of the two-parameter hyperbolic tangent switching function allows modeling of the $CH_3 + H$ recombination with an essentially zero temperature coefficient around room temperature, which then becomes increasingly more negative at higher temperatures, and at the same time return a 300 K value of $\langle k_{rec,\infty} \rangle$ that is close to experiment, as shown in Table I and Figure 7.

The problems associated with extrapolating experimental data to high pressures are notorious, so that it is perhaps unwise to set too much store by the actual value of the experimentally determined temperature coefficient of k_∞. If the *sign* of the temperature coefficient of $CH_3 + H$ as deduced from experiment is in error due to extrapolation problems, it is not clear why this extrapolation should lead to an error of *sign* in the $CH_3 + H$ association and not in the case $CH_3 + CH_3$. In general, $\langle k_{rec,\infty} \rangle$ in association reactions is likely to follow a more complicated temperature dependence than a simple T^n law. For example, in the $CH_3 + CH_3$ association, n varies from –0.1 in the 300 K range to –0.8 in the 1000 K range. It is therefore plausible that the temperature dependence of the association $CH_3 + H$, like most radical associations, should follow a power law with n that also becomes more negative as temperature increases, but one that starts out as $n \approx 0$ (or perhaps slightly positive) in the 300–400 K range. This would reconcile both the recent low-temperature data of Pilling and the two cited reviews which presumably gave greater weight to high-temperature dissociation data. Hopefully future experiments will resolve this conundrum.

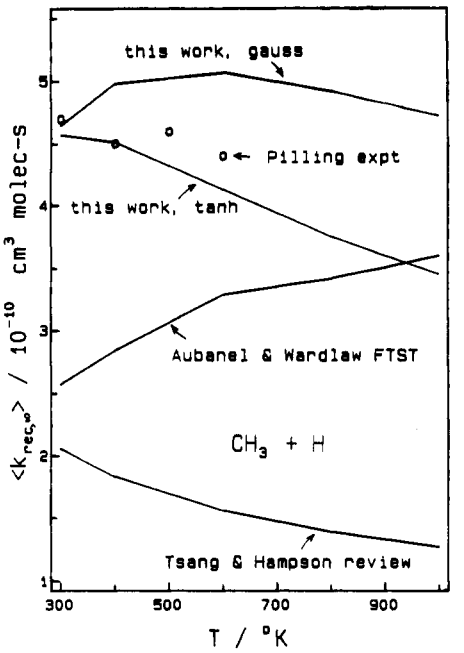

Figure 7. Summary of data on the temperature dependence of $\langle k_{rec,\infty} \rangle$ for the association $CH_3 + H$. Experiment: Tsang and Hampson review;[15] Pilling expt (circles, ref 14). Theory: Aubanel and Wardlaw FTST;[20] this work (Table I).

The data shown in Figure 1 throw an interesting light on the question of the origin of the negative temperature coefficient in an association reaction. If the state count for the transition state, as a function of distance along the reaction coordinate, evolves as shown in the top panel of Figure 1 (e.g., using the simple exponential switching function (eq 3), calculations by the present variational routine produce invariably $\langle k_{rec,\infty} \rangle$ with a basically *positive* temperature coefficient over a large temperature range, regardless of any reasonable interfragment potential. On the other hand, if the same state count evolves as shown in the bottom panel of Figure 1 (e.g., using the Gaussian or hyperbolic tangent switching function), the temperature coefficient of $\langle k_{rec,\infty} \rangle$ will be essentially *negative*.

This suggests that the temperature coefficient depends primarily on the switching function which governs the approach of the system to the final state: if the approach is "early" (Figure 1, top), the transition state will be looser (at larger internuclear distance), and $\langle k_{rec,\infty} \rangle$ will have usually a positive temperature coefficient; if the approach is "late" (Figure 1, bottom), the transition state will be tighter (at shorter internuclear distance), and the temperature coefficient of $\langle k_{rec,\infty} \rangle$ will be usually negative. The present calculations (and other as-yet unpublished calculations on other radical recombinations) show that in general the "late" approach is the preferred one.

In the face of such radically different "early" and "late" switching functions, the details of the interfragment potential play only a secondary role. For example, with the "early"-type switching function, it is not possible to reverse the positive temperature coefficient of $\langle k_{rec,\infty} \rangle$ by making an "adjusted" Morse potential more attractive so as to produce a $\langle k_{rec,\infty} \rangle$ with a sufficiently negative temperature coefficient of the correct magnitude. On the other hand, a "better" potential would clearly offer a means for fine-tuning the results in conjunction with a late-type switching function.

11. Conclusions

It should be emphasized that the present calculation requires only the molecular parameters of reactant and products as sole input and then merely interpolates between reactant and product state counts, using a Morse function for the potential of the separating fragments, likewise obtained from reactant parameters. While the interpolation idea is common to many variational

(23) Wagner, A. F.; Wardlaw, D. M. *J. Phys. Chem.* **1988**, *92*, 2462.

schemes,[24] they differ in approach and complexity. The relative success of the present simple scheme is due to the way the combined partition function inversion procedure plus switching function describe—by all accounts fairly correctly—the most complicated event, which is the progressive conversion of a reactant transitional vibrational mode first into a hindered, and then a free, rotor in the products.

Admittedly the description of this key event neglects completely the coupling of the angular momentum of transitional rotors with the overall rotational angular momentum to give the conserved total angular momentum, a coupling that by contrast the FTST model treats explicitly. Nevertheless the present simplified treatment yields comparable results, which illustrates that the multiple averaging that leads to a thermal rate constant washes out so much of the microscopic detail that one can make do with limited information and very simple representation.

There are, to be sure, adjustable parameters: one in the Gaussian switching function, two in the hyperbolic tangent. The present routine can readily accommodate different switching functions and/or potential functions obtained, e.g., from ab initio calculations, which would eliminate in principle (but perhaps not in practice) all adjustable parameters. (Note that even the FTST cannot do without an adjustable parameter.)

The Gaussian switching function (eq 20) has the advantage that it uses a single adjustable parameter, which (in units of $Å^{-1}$) comes close to about 0.25 β(Morse) in the two cases examined so far. It remains to be seen if it is endowed with the same apparent universality as the parameter α in the exponential switching function of eq 3 used in other variational schemes.[1,9]

The two-parameter hyperbolic tangent switching function (eq 19) offers obviously a greater flexibility insofar as modeling experimental results is concerned, but no greater insight into the dynamics of the process since there is no recipe for determining the constants a and b in any particular case, beyond the observation that in general, but only very approximately, $a \approx 0.2\beta$(Morse), after conversion into units of $Å^{-1}$ and $b \approx \beta$(Morse).

On the surface, the steepest descents routine described in section 4 does not have much to recommend it for speed since it involves a transcendental equation that must be solved by iteration. However each final z_2 serves as input for iteration at the next r, generally 0.1 Å or less apart. As a result, the various final z_2 are not too different, so that two, or at most three, iterations are sufficient.

The implementation as shown in section 4 is for separable harmonic oscillators, but it can be extended to separable Morse oscillators if the requisite data are available, at a modest increase in complexity.[25]

This partition function inversion approach should be useful primarily for microcanonical variational calculation within the framework of conventional RRKM treatment destined to model the falloff of thermal rate constants, on molecules where available information is limited and/or more sophisticated calculations would be prohibitive. Work on halogen-substituted methanes of atmospheric interest is currently in progress.[26]

Registry No. CH_3, 2229-07-4; H, 12385-13-6.

(24) Greenhill, P. G.; Gilbert, R. G. *J. Phys. Chem.* **1986**, *90*, 3104.

(25) Forst, W.; Prasil, Z. *J. Chem. Phys.* **1970**, *53*, 3065. Huy, L. K.; Forst, W.; Prasil, Z. *Chem. Phys. Lett.* **1971**, *9*, 476.

(26) Forst, W.; Caralp, F. *J. Chem. Soc., Faraday Trans.*, submitted for publication.

One-Dimensional Triplet Energy Migration in Columnar Liquid Crystals of Octasubstituted Phthalocyanines

Dimitra Markovitsi,* Isabelle Lécuyer,

CEA, Centre d'Etudes de Saclay, DSM/SCM/CNRS URA 331, Laboratoire de Photochimie, 91191 sur Yvette Cédex, France

and Jacques Simon

ESPCI-CNRS, UA 429, Laboratoire de Chimie et Electrochimie des Matériaux Moléculaires, 10, rue Vauquelin, 75231 Paris Cédex 05, France *(Received: July 24, 1990; In Final Form: November 9, 1990)*

Time-resolved absorption spectroscopy has been used to study laser-induced triplet excitons of the octakis(alkoxymethyl) metal-free and zinc phthalocyanines $\{(C_{12}OCH_2)_8PcH_2$, $(C_{18}OCH_2)_8PcH_2$ and $(C_{12}OCH_2)_8PcZn\}$ in their crystalline and columnar liquid-crystalline phases. The triplet states have been characterized by their absorption spectra and their decay kinetics. At early times, the triplet state population varies as $t^{-1/2}$, which is characteristic of diffusion-limited one-dimensional triplet–triplet annihilation. The long-time decays are well described by a model of random walk on a linear chain containing traps. The incoherent exciton path length between two successive defect sites is on the order of a micrometer, and it could be correlated with the size of the microdomains. The values of the exciton hopping time (0.4–68 ps) determined from the short-time decay kinetics are in agreement with those determined independently from the long-time behavior of the triplet decay. The exciton diffusion coefficients determined for the columnar mesophases are found to be higher than those observed in the crystalline phases of the same compounds, consistent with a more efficient energy migration in the liquid crystal than in the crystal.

Introduction

One-dimensional energy migration has received considerable attention. Numerous theoretical works describe the properties of quasi-one dimensional incoherent excitons.[1-8] Experimentally, such excitons have been detected by studying luminescence from crystals of 1,4-dibromonaphthalene,[9] 1,2,4,5-tetrachlorobenzene,[2,10]

(1) Montroll, E. W. *Phys. Soc. Jpn.* **1969**, *26*, 6.

(2) Dlott, D. D.; Fayer, M. D.; Wieting, R. D. *J. Chem. Phys.* **1978**, *69*, 2752.

(3) Movaghar, B.; Sauer, G. W.; Würtz, D. *J. Stat. Phys.* **1982**, *27*, 473.

(4) Torney, D. C.; McConnell, H. M. *J. Phys. Chem.* **1983**, *87*, 1941.

(5) Redner, S.; Kang, K. *Phys. Rev. Lett.* **1983**, *51*, 1729.

(6) Blumen, A.; Klafter, J.; Zumofen, G. *Optical Spectroscopy of Glasses*; Zschokke, I., Ed.; D. Reidel Publishing Co.: Dordrecht, Holland, 1986; pp 199-265.

0022-3654/91/2095-3620$02.50/0